NANO LETTERS

pubs.acs.org/NanoLett

Letter

pH-Controlled Resettable Modular DNA Strand-Displacement Circuits

Xiaoyun Sun,[‡] Dongbao Yao,*[,‡] and Haojun Liang*

Cite This: *Nano Lett.* 2023, 23, 11540−11547

Read Online

ACCESS | Metrics & More | Article Recommendations | Supporting Information

ABSTRACT: Sophisticated dynamic molecular systems with diverse functions have been fabricated by using the fundamental tool of toehold-mediated strand displacement (TMSD) in the field of dynamic DNA nanotechnology. However, simple approaches to reset these TMSD-based dynamic systems are lacking due to the difficulty in creating kinetically favored pathways to implement the backward resetting reactions. Here, we develop a facile proton-driven strategy to achieve complete resetting of a modular DNA circuit by integrating a pH-responsive intermolecular CG-C$^+$ triplex DNA and an i-motif DNA into the conventional DNA substrate. The pH-programmed strategy allows modular DNA components to specifically associate/dissociate to promote the forward/backward TMSD reactions, thereby enabling the modular DNA circuit to be repeatedly operated at a constant temperature without generating any DNA waste products. Leveraging this tractable approach, we further constructed two resettable DNA logic gates used for logical computation and two resettable catalytic DNA systems with good performance in signal transduction and amplification.

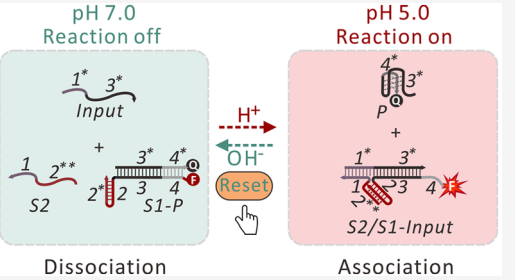

KEYWORDS: *toehold-mediated strand displacement, resettable modular DNA circuit, pH-responsive intermolecular triplex, i-motif, detachable substrate*

Possessing the unique programmability and structural predictability, DNA has increasingly been utilized to fabricate sophisticated self-assembled nanostructures and programmable molecular systems with dynamic behaviors by exploiting Watson−Crick base-pairing rules.[1,2] Most importantly, the emergence of toehold-mediated strand displacement (TMSD) in the field of dynamic DNA nanotechnology,[3] a reaction wherein an invading strand hybridizes with a single-stranded domain (called toehold) to displace one or more prehybridized strands through branch migration (BM) in a DNA substrate, has offered a powerful engineering tool in constructing dynamic DNA nanodevices.[4] These TMSD-based dynamic molecular systems with diverse functions have included DNA walkers that move along predesigned tracks,[5−7] DNA oscillators,[8] single-molecule DNA navigators,[9] toehold switches for the regulation of gene expression,[10] and a cartwheeling DNA acrobat.[11] Among them, DNA circuits with molecular information processing ability in particular have exhibited prolific and inventive designs and have been widely applied for logical computation,[12−16] molecular neural networks,[17,18] signal amplification,[19−21] catalytic assembly of colloidal nanoparticles,[22−24] self-assembly of DNA nanostructures,[25,26] biosensors,[27−29] and cell imaging.[30,31]

To date, however, it is unfortunately hard to construct TMSD-based dynamic molecular systems with reset functions owing to the difficulty in creating viable kinetic pathways to trigger the backward resetting reactions once the forward TMSD reactions reached equilibrium states. This drawback has undoubtedly impeded the application potential of these TMSD-based dynamic molecular systems in terms of reprogrammability and reusability. Moreover, the accumulated irreversible waste products generated during running of these nonresettable molecular systems caused a huge waste of DNA materials. Recently, the renewable TMSD-based DNA circuits reported by Reif et al. can be reused by addition of extra DNA strands;[32,33] however, large amounts of DNA wastes were accumulated during the repeated operation processes. In addition, the azobenzene molecules were introduced into the TMSD reactions to try to reset the DNA circuits,[34−36] but these photoresponsive systems cannot be reset completely since the azobenzene-initiated duplex dehybridization could not achieve perfect yield in reality. To further circumvent this issue, Shih et al. constructed associative TMSD-based resettable DNA nanodevices controlled by temperature cycling;[37] Song et al. implemented the single-molecule resettable DNA computing via magnetic tweezers;[38] and Walther and co-worker developed a transient TMSD-based self-resettable circuit with programmable lifetimes driven by

Received: August 29, 2023
Revised: December 7, 2023
Accepted: December 8, 2023
Published: December 12, 2023

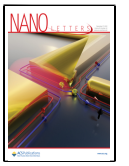

https://doi.org/10.1021/acs.nanolett.3c03265
Nano Lett. 2023, 23, 11540−11547

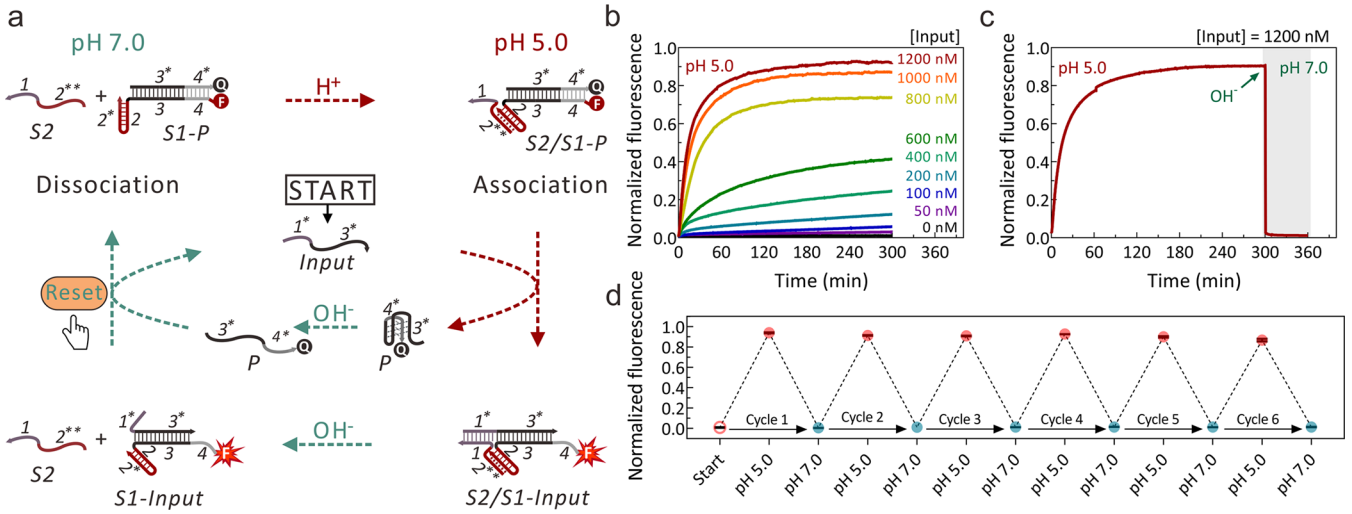

Figure 1. pH-controlled resettable modular DNA circuit. (a) Schematic illustration of the resettable DNA circuit controlled through cyclic pH changes. (b) Real-time fluorescence kinetics of the pH-responsive TMSD reactions with the addition of different concentrations of Input at pH 5.0. (c) Real-time changes in the fluorescent signal intensity of the pH-controlled resettable modular DNA circuit from pH 5.0 to 7.0 by adding 1.5 μL of 1 M NaOH after 300 min of reaction. (d) Reversible fluorescent signal changes demonstrating the good resettability of the pH-controlled modular DNA circuit by cyclically varying the pH between 5.0 and 7.0 in the presence of 1200 nM of Input. All experiments were performed at 37 °C, [S1-P] = 200 nM, and [S2] = 800 nM.

the ATP-fueled ligation/restriction network.[39] Although these TMSD-based molecular systems can be reset completely, the assistance of specialized instruments or specific enzymes was necessary.

Given the current predicament, in the present work, we demonstrate a facile and adaptable design of a completely resettable modular DNA circuit driven by protons at constant temperature by integrating the pH-controlled intermolecular CG-C$^+$ triplex structure[40−43] (for reversibly bridging the modular substrate) and the DNA i-motif[44−46] (as a trigger for the backward resetting reaction and the reversible signal reporter) with the conventional TMSD-based DNA circuit. In our strategy, the collaboration of formation/destruction of the pH-responsive intermolecular triplex and i-motif DNA structures in the modular DNA circuit allows the realization of the forward and backward TMSD reactions at pH 5.0 and 7.0, respectively. Leveraging this tractable pH-controlled approach that allows modular DNA components to programmatically assemble and disassemble to promote the forward and backward TMSD reactions, we further construct two resettable DNA logic gates and two resettable catalytic DNA systems.

DESIGN OF A pH-CONTROLLED RESETTABLE MODULAR DNA CIRCUIT

For the construction of the DNA substrate, we adopted the "detachable substrate" strategy proposed previously by our group[43] by embedding an intermolecular CG-C$^+$ triplex DNA structure (composed of a cytosine-rich triplex-forming strand and a CG duplex through Hoogsteen interactions, and the average p*K*a of cytosines in triplex DNA is ∼6.5)[47] into the traditional "linear substrate". The detachable substrate is composed of two pH-responsive modules: a BM complex named S1-P and a single-stranded toehold named S2 (Figure 1a). The reversible association and dissociation processes of the pH-responsive intermolecular triplex DNA structure (2**/2−2*) adopted in the detachable substrate design were verified through the fluorescence kinetics measurements when the pH was alternatively changed between 5.0 and 7.0 (see Figure S1 for details).

As depicted in Figure 1a, at initial pH 7.0 (neutral condition), S1-P cannot associate with S2, yielding a stable system in the presence of Input. Once the pH is tuned to pH 5.0 (acidic condition), the triplex-forming domain (2**) in S2 can bind with the CG hairpin (2−2*) of S1-P to form an intermolecular CG-C$^+$ triplex structure through Hoogsteen interactions. Thus, S2 and S1-P are bridged together to generate a complete substrate (S2/S1-P). Then, domain 1* of Input can interact with the complementary toehold (domain 1) in S2 to displace the prehybridized Protector strand P (domain 3*-4*) in S1-P through BM to initiate the forward TMSD reaction, while yielding a complex called S2/S1-Input. Notably, the released strand P containing four stretches of cytosines will fold into an inactive four-stranded DNA structure called i-motif[44−46] (held together by hemiprotonated and intercalated cytosine base pairs under acidic conditions) to prevent the rebinding between P and S2/S1-Input, thereby further promoting the completion of the forward TMSD reaction. Meanwhile, the release of P from S1-P leads to the generation of a fluorescent signal to characterize the forward TMSD reaction, as S1 is labeled with a pH-insensitive dye Alexa Fluor 488 at the 5′ end, and P is labeled with a corresponding quencher BHQ1 at the 3′ end. If the pH is restored to 7.0 again, the conformation of the pH-sensitive P will change from a closed i-motif into a floppy random-coil structure, and the pH-controlled intermolecular CG-C$^+$ triplex structure for bridging S1 and S2 will be destructed simultaneously. Then, the forward invading toehold (domain 1) of module S2 will further dissociate from its complementary domain (domain 1*) on S1-Input due to the thermodynamic instability of the short duplex DNA at 37 °C, thus resulting in the complete dissociation of S2 from S2/S1-Input at pH 7.0. Subsequently, domain 4* of unfolded strand P binds with the backward invading toehold (domain 4) to displace Input to regenerate S1-P through the backward TMSD reaction. By utilizing the dynamic pH cycling method, the pH-controlled

https://doi.org/10.1021/acs.nanolett.3c03265
Nano Lett. 2023, 23, 11540−11547

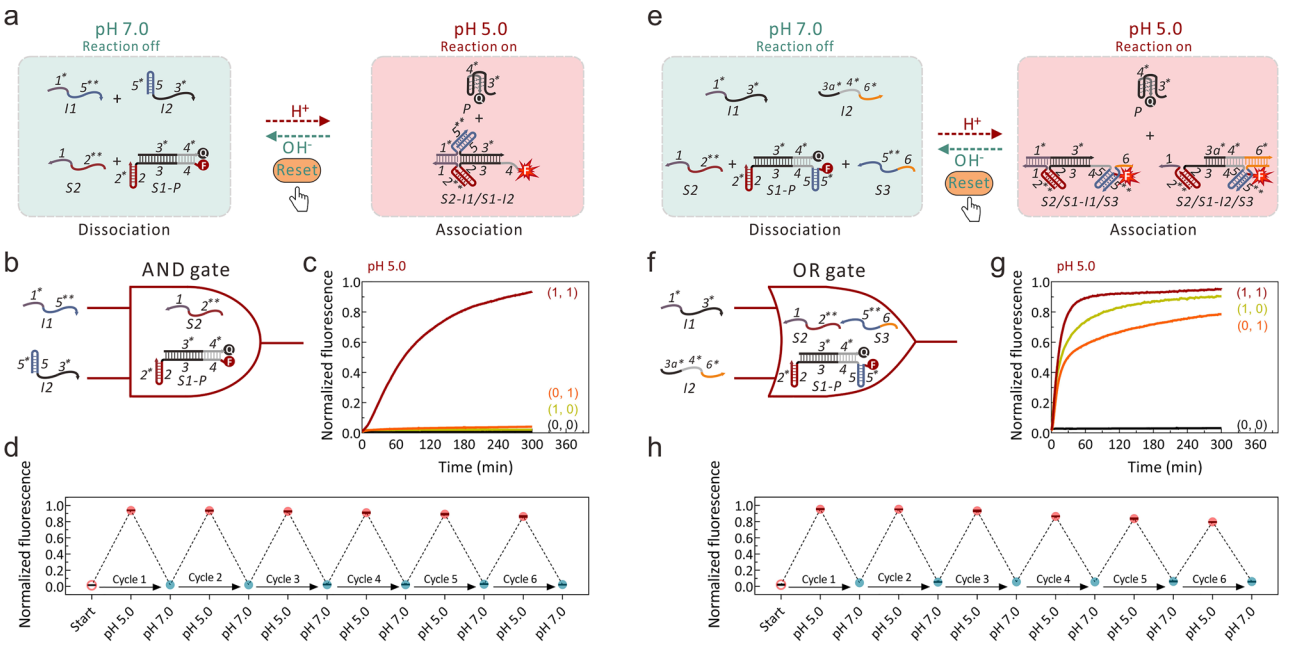

Figure 2. pH-controlled resettable DNA computing circuits. (a) Brief scheme of the resettable AND gate system. (b) Symbol for the AND gate. (c) Kinetic curves representing the signal outputs of the AND gate at pH 5.0 ([I1] = 1200 and [I2] = 1200 nM, respectively). (d) Reversible fluorescent signal changes demonstrating the resettability of the AND gate system with the addition of both I1 (1200 nM) and I2 (1200 nM). For the AND gate, [S1-P] = 200 nM and [S2] = 800 nM. (e) Brief scheme of the resettable OR gate system. Note that S1-P, i.e., the reversible fluorescence reporter for characterization the output signal in the OR gate, is formed by hybridization of the double-loop S1 (labeled with a pH-insensitive dye Alexa Fluor 488 at the 5′ end) and the i-motif P (labeled with a corresponding quencher BHQ1 at the 3′ end). (f) Symbol for the OR gate. (g) Kinetic curves representing the signal outputs of the OR gate at pH 5.0 ([I1] = [I2] = 2400 nM). (h) Resettability measurement of the OR gate system in the presence of 2400 nM of I1 and 2400 nM of I2 simultaneously. For the OR gate, [S1-P] = 200 nM, [S2] = 800 nM, and [S3] = 800 nM. All experiments were performed at 37 °C.

modular DNA circuit can be completely reset to the initial state without generating any DNA wastes at constant temperature. Note that the formation of the inactive state of P (i-motif) at pH 5.0 and the fast and complete TMSD reaction that occurred between S1-Input and the unfolded P at pH 7.0 were proved in Figure S2, indicating that P has good pH responsiveness as the signal reporter and good reaction ability as the trigger of the backward resetting reaction in our pH-controlled DNA circuit.

OPERATION OF THE pH-CONTROLLED RESETTABLE MODULAR DNA CIRCUIT

We first optimized the molar ratio of S1-P and S2 to comprise the detachable substrate at pH 5.0 (Figure S3). Then, at pH 5.0, the forward TMSD reaction performance of the pH-controlled modular DNA circuit was investigated with the addition of different amounts of Input (Figure 1b). It was found that there was an obvious improvement in reaction efficiency with an increase of the Input concentration (from 50 to 1200 nM). The forward reaction approached equilibrium in 300 min and resulted in a high product yield up to ~92% in the presence of 1200 nM Input, indicating the good reaction performance of the pH-controlled modular DNA circuit. In contrast, at initial pH 7.0, no fluorescent signal was observed even when the Input concentration was up to 1200 nM (Figure S4). As a control, a pH-insensitive modular circuit was designed by substituting the triplex-forming domain (domain 2**) in S2 with a random sequence unable to associate with S1-P to form a complete substrate under acidic conditions (Figures S5 and S6), which demonstrated the high specificity of our pH-controlled modular DNA circuit.

We then explored the resettability of the pH-controlled modular DNA circuit by cyclically tuning the pH value between 5.0 and 7.0. As shown in Figure 1c, upon addition of 1200 nM Input in the total reaction volume of 200 μL at initial pH 5.0, the forward TMSD reaction signal reached the maximum after 300 min. Then, 1.5 μL of 1 M NaOH was added to make the pH of the reaction solution change to 7.0, and the fluorescent signal of the system was restored to the minimum very quickly (took less than 1 min), indicating the complete resetting of the modular DNA circuit resulting from the backward TMSD reaction (cycle 1). Then, by introducing 1.5 μL of 1 M HCl to bring the pH back to 5.0, the DNA circuit can be reactivated again (Figure 1d). By cyclically tuning the pH value of the system in this manner after each TMSD reaction, it was found that the pH-controlled modular DNA circuit can be operated repeatedly 6 times (cycles 1 to 6) with only small loss in reactivity without generating any DNA wastes (Figure 1d). This result fully demonstrated the good resettability and high dynamic programmability of our pH-controlled resettable modular DNA circuit.

RESETTABLE DNA LOGIC SYSTEMS

TMSD-based DNA logic gates have exhibited prolific and creative designs and have been widely applied in biosensing, diagnosis, and digital computation.[14] In addition, the combination and cascading of different TMSD-based DNA logic gates can be used to build multilayer and scaled-up digital logic circuits that perform higher-level computing functionality.[12,48,49] However, most of these DNA logic systems cannot be reset after operations, which limits their potential in the

https://doi.org/10.1021/acs.nanolett.3c03265
Nano Lett. 2023, 23, 11540−11547

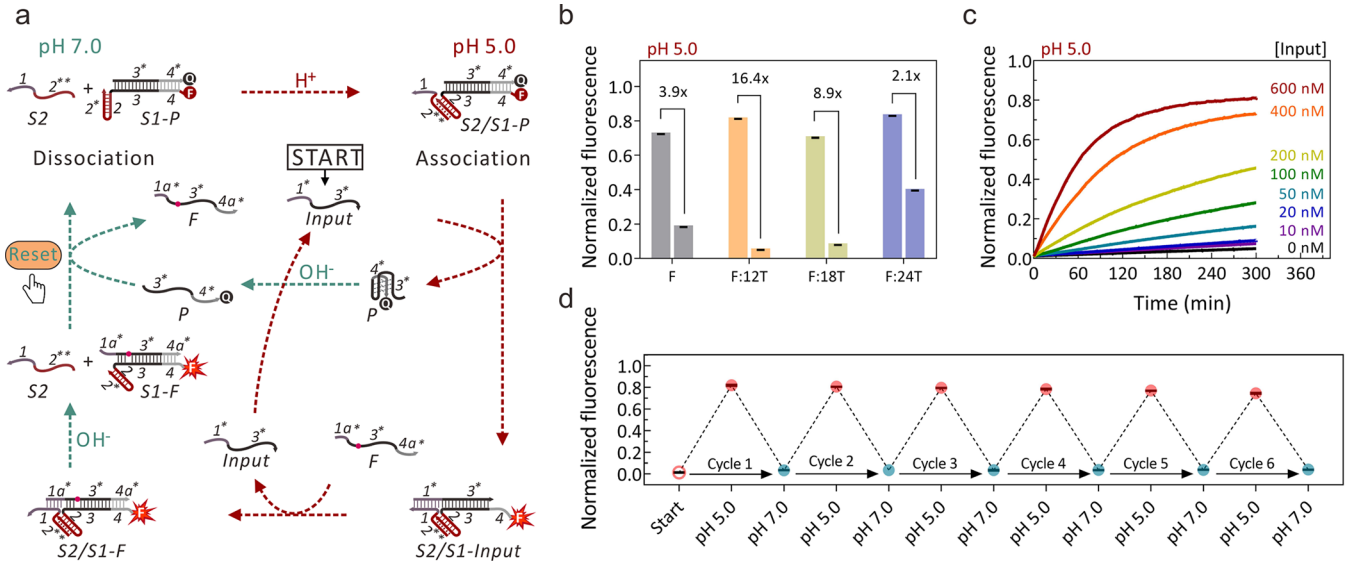

Figure 3. Resettable modular catalytic DNA circuit. (a) Graphical representation of the pH-controlled resettable catalytic DNA circuit. (b) Performances of the normal F strand and different types of F strands (4 μM) with single-base mismatch at different positions (F:12T, F:18T, and F:24T, respectively) in the resettable catalytic DNA circuit in the presence (left) or absence of 600 nM Input (right). (c) Real-time fluorescence kinetics of a catalytic DNA circuit under varied concentrations of Input at pH 5.0. (d) Resettability demonstration of the modular catalytic DNA circuit in the presence of 600 nM of Input. All experiments were performed at 37 °C, [S1-P] = 200 nM, and [S2] = 800 nM. In (c) and (d), [F:12T] = 4 μM.

construction of sophisticated DNA digital logic systems more closely to the semiconductor circuits in function.

Given that, we constructed a resettable AND logic gate based on the pH-controlled resettable TMSD reactions. The two inputs (Input 1 and Input 2) in this AND gate are designed by splitting the original Input used in the above resettable modular DNA circuit into two intermediate strands from the position connecting the toehold and BM domain (Input 1′ and Input 2′) first and then inserting an intermolecular pH-responsive CG-C$^+$ triplex DNA structure (Figure S7). As shown in Figure 2a,b, at pH 5.0, Input 1 (called I1 for short) can associate with Input 2 (called I2 for short) to form a triplex DNA complex (I1/I2) possessing the same function as the Input strand. If the pH is tuned to 7.0 after the logic operation, I1 and S2 will dissociate from the product (S2-I1/S1-I2), and meanwhile, P will unfold to trigger the backward TMSD reaction to reset the AND gate system (the detailed reaction scheme can be found in Figure S8). As expected (Figure 2c), the AND gate system generated the output fluorescent signal by adding a mixture containing 1200 nM I1 and 1200 nM I2 (1, 1), whereas no output fluorescent signal was obtained with the addition of only I1 (1, 0), or only I2 (0, 1), or in the absence of both input strands (0, 0). Similarly, the resettability of the AND gate was demonstrated through repeating the AND logic operations for 6 times by cyclically tuning the pH of the solution between 5.0 and 7.0 in the presence of both I1 and I2 (1, 1) (Figures 2d and S10). As predicated, there were no obvious fluorescent responses for the other three input conditions (Figure S11).

Then, we designed a resettable OR logic gate on the basis of the above pH-responsive modular DNA circuit by integrating another intermolecular pH-responsive CG-C$^+$ triplex DNA structure into the two-module detachable substrate (S2/S1-P). As shown in Figure 2e,f, the constructed detachable substrate in the OR gate is composed of three modules: S1-P, S2, and S3. Among them, S2 and S3 are single-stranded toehold modules with different triplex-forming domains (2** for S2 and 5** for S3), respectively, while S1-P is the BM module with two different CG hairpin structures (2−2* and 5−5*) at both ends that can interact with S2 and S3 under acidic conditions (the detailed reaction scheme is shown in Figure S12). As shown in the experiment, either I1 (1, 0) or I2 (0, 1), as well as their mixture (1, 1), can trigger output signals in the OR logic system (Figure 2g). Moreover, the OR gate also exhibited good resettability under these three input conditions (Figures 2h and S13 and S14).

RESETTABLE CATALYTIC DNA CIRCUIT

Analogous to catalytic reactions in chemistry, DNA strands can act as catalysts to fuel DNA-based molecular systems through a series of TMSD reactions. The catalytic DNA systems have included the entropy-driven networks catalyzed by DNA,[19,50] DNA neural networks,[18] DNA-based digital logic circuits,[48] and signal amplification networks for molecular diagnostics.[51,52] However, these catalytic DNA systems are limited in reusability due to the irreversible consumption of reactants and accumulation of DNA wastes. To address this dilemma, we constructed a fuel strand DNA-powered resettable catalytic DNA circuit based on the above pH-controlled resettable modular DNA circuit.

The resettable catalytic DNA circuit is illustrated in Figure 3a. The system remains stable in the presence of Input (acts as catalyst) and Fuel (F) under the initial neutral conditions. If the pH is changed from 7.0 to 5.0, S1-P and S2 can associate with each other to assemble into a complete substrate first. Input can then bind with the toehold (domain 1) on S2 to trigger the forward TMSD reaction and release the fluorescent signal while generating the intermediate product S2/S1 Input. Subsequently, the domain 4a* of F can bind with the backward toehold of domain 4 in S2/S1 Input to start a new round of TMSD reactions, thereby displacing Input and yielding a final product S2/S1-F. The F strand is employed to sustain the

https://doi.org/10.1021/acs.nanolett.3c03265
Nano Lett. 2023, 23, 11540−11547

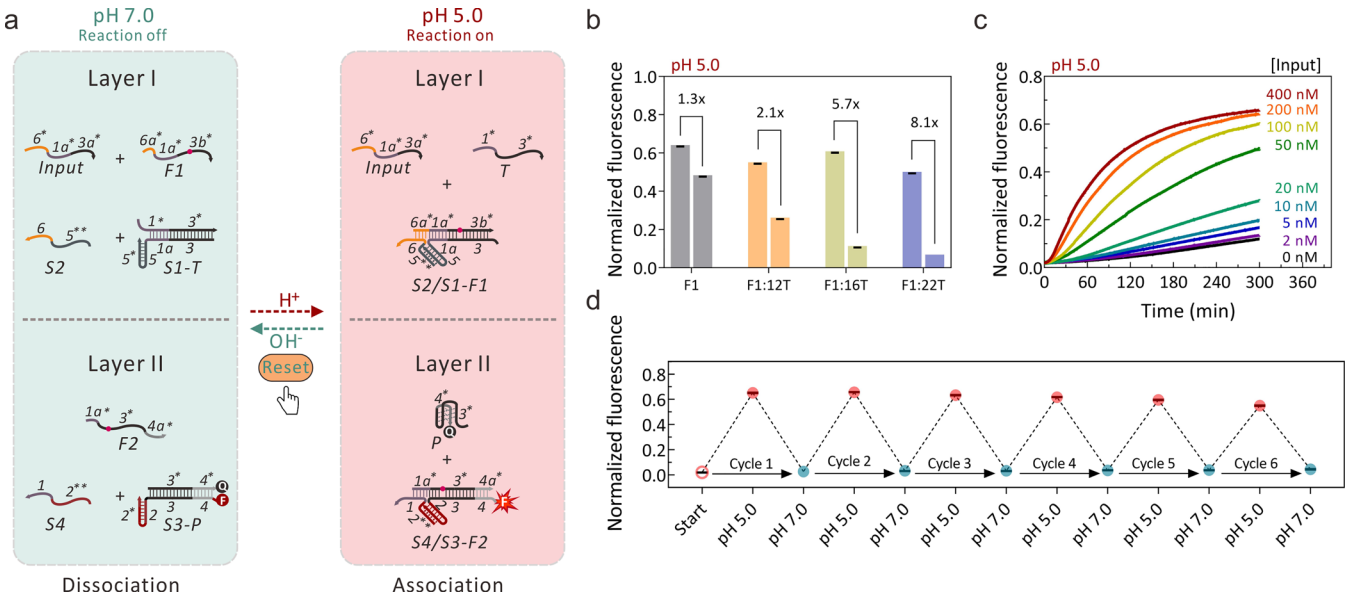

Figure 4. Resettable two-layer cascaded catalytic DNA circuit. (a) Brief scheme of the pH-controlled resettable two-layer cascaded catalytic DNA circuit. (b) Performances of normal Fuel strand F1 (1.2 μM) and different types of Fuel strands (1.2 μM) with single-base mismatch at different positions (F1:12T, F1:16T, and F1:22T, respectively) involved in layer I of the two-layer catalytic DNA circuit in the presence or absence of 100 nM Input. (c) Real-time fluorescence kinetics of the two-layer catalytic DNA circuit in the presence of varied concentrations of Input at pH 5.0. (d) Resettability demonstration of the two-layer modular catalytic DNA circuit in the presence of 200 nM of Input. All experiments were performed at 37 °C, [S1-T] = 600 nM, [S2] = 1200 nM, [S3-P] = 200 nM, [S4] = 800 nM, and [F2] = 1.2 μM. In (c) and (d), [F1:16T] = 1.2 μM.

continuous running of the catalytic circuit through providing driving force. Therefore, the released Input is reused to restart further TMSD reactions in the catalytic circuit. If the pH is restored to 7.0 after the forward TMSD reaction finishes, S2 will dissociate from S2/S1-F, and P will bind with the unhybridized single-stranded part of domain 4 on S1-F to initiate the backward resetting reaction, leading to the complete reset of the catalytic circuit.

We first optimized the design of F in the resettable catalytic circuit at pH 5.0 (Figure S15). According to previous reports, a mismatched F could improve the performance of the catalytic DNA circuits.[22,53,54] To reduce the signal leakage and improve the driving force of F, we designed three types of F strands with a single-base mismatch at different positions, named F:12T, F:18T, and F:24T, respectively. Compared with the other two mismatched F designs, the catalytic system exhibited the lowest signal leakage (5%) and acceptable reaction efficiency (81.2%) in the presence of F:12T (Figure S15). The S/N value for F:12T was as high as 16.4 after calculation (Figure 3b). Considering that there is a substantial overlap in the DNA sequences between the normal F strand and the i-motif strand (P) adopted in the resettable catalytic circuit, we speculated that the normal F strand may fold into a secondary structure with relatively low reactivity at pH 5.0, whereas the single-base mismatch in F:12T can prevent the formation of a secondary structure. Therefore, the design of F:12T with a single-base mismatch not only helps to reduce the signal leakage but also improves the efficiency of the TMSD reaction. Thus, the design strategy of the mismatched F strand in the resettable catalytic DNA circuit was determined as F:12T.

Subsequently, we investigated the performance of the resettable catalytic DNA circuit with the addition of different concentrations of Input at pH 5.0. As shown in Figure 3c, a series of remarkable fluorescent signal outputs were observed by increasing the concentration of Input gradually (from 0 to 600 nM). In particular, a distinguishable signal was achieved in the presence of 10 nM Input, constituting a 5-fold improvement in signal transduction ability relative to the above noncatalytic DNA circuit in Figure 1b. Lastly, the good resettability of the modular catalytic DNA circuit was proved through the pH cycling experiment (Figures 3d and S16).

RESETTABLE TWO-LAYER CASCADED CATALYTIC DNA CIRCUITS

To further demonstrate the flexibility and expandability of our pH-controlled modular catalytic DNA circuit, we intended to construct two-layer cascaded catalytic DNA circuits with resettability. To this end, another pH-controlled modular catalytic DNA circuit (serves as layer I) was integrated with the above resettable catalytic DNA circuit (serves as layer II) to constitute a two-layer catalytic DNA system, and these two modular DNA circuits were connected together through a single strand called Trigger (T) released from layer I (Figure 4a). The operating mechanism of the two-layer cascaded DNA circuits is depicted in detail in Figure S17. At pH 7.0, all pH-responsive modules are unable to assemble due to their inactivation, thereby enabling the good stability of the whole cascaded system in the presence of Input. Once the pH is changed from 7.0 to 5.0, the pH-responsive modular components in layer I (S1-T and S2) and layer II (S3-P and S4) will assemble into complete substrates (S2/S1-T and S4/S3-P) through Hoogsteen interactions, respectively. Input can combine with its toehold (domain 6) on S2/S1-T in layer I to displace T through the TMSD reaction, while yielding an intermediate complex called S2/S1 Input having a newly generated toehold (at the end of domain 3). Then, the Fuel strand of layer I (F1) binds to the new toehold to initiate a new round of TMSD reaction, leading to the displacement of Input and the generation of product called S2/S1-F1. The released Input can restart the next round of the TMSD reaction in the modular DNA circuit in layer I. Meanwhile, the

https://doi.org/10.1021/acs.nanolett.3c03265
Nano Lett. 2023, 23, 11540−11547

continuously released T from layer I can initiate and catalyze the running of the modular DNA circuit in layer II, thereby resulting in the release of i-motif P and the generation of the fluorescent signal. If the pH is restored to 7.0 again, the strand P will unfold from the i-motif state, and the toehold modules of S2 and S4 will dissociate from S2/S1-F1 in layer I and S4/S3-F2 in layer II (note that F2 is the Fuel strand used in layer II), respectively. Then, T and P will initiate the backward TMSD reactions in layer I and layer II, respectively, thereby displacing F1 and F2 and resulting in the formation of S1-T and S3-P to finally realize the complete reset of the cascaded system (Figures 4a and S17).

Similarly, to reduce the signal leakage and improve the performance of the cascaded DNA circuits, the mismatch-strand strategy was still adopted in designing F1 and F2 here. Note that the single-base mismatch position of F2 in layer II was kept the same as that of the above one-layer catalytic circuit (i.e., F:12T). The design of F1 in layer I was implemented by mutating the sequence at different positions (named F1:12T, F1:16T, and F1:22T, respectively). After investigation of the performances of these mutated F1 strands in the cascaded system at pH 5.0 (Figures 4b and S18), F1:16T was chosen to be used in the following studies in the cascaded catalytic system.

We next tested the performances of the two-layer cascaded catalytic DNA circuits with the addition of different amounts of Input (from 0 to 400 nM) at pH 5.0. As shown in Figure 4c, the fluorescent signal obviously increased with increasing the concentration of input, indicating the continuous improvement of the reaction efficiency of the cascaded system. Notably, the fluorescent signal generated in the presence of 2 nM of Input was distinguishable from the background signal (Figure 4c, "0 nM" line), achieving 5-fold improvement in signal transduction ability relative to the one-layer catalytic DNA circuit in Figure 3c and 25-fold improvement relative to the noncatalytic DNA circuit in Figure 1b, respectively. Finally, the good resetting ability of the pH-controlled cascaded catalytic system was demonstrated by cyclically changing the pH between 5.0 and 7.0 (Figures 4d and S20).

In summary, by embedding the pH-responsive intermolecular CG-C^+ triplex DNA structure and the pH-responsive i-motif DNA strand in the conventional linear DNA substrate, we developed a simple and robust strategy to achieve complete resetting of TMSD-based modular DNA circuits at a constant temperature without generating any DNA wastes. Given such a high degree of modularity and simplicity of our pH-controlled modular strategy, it should be possible to construct many other sophisticated dynamic molecular systems with programmable resettable behaviors by stacking more pH-responsive modular components in the TMSD-based reaction networks. In addition, by integrating with other building blocks (e.g., DNA-functionalized colloidal nanoparticles[23,24,55] and DNA bricks[56]), our pH-controlled modular strategy should be of great potential in building resettable three-dimensional DNA assembly structures and reprogrammable colloidal crystals. Moreover, implementing our approach in DNA-based sensors will find applications in the reusability and recyclability of molecular diagnostic devices.

■ ASSOCIATED CONTENT

Supporting Information

The Supporting Information is available free of charge at https://pubs.acs.org/doi/10.1021/acs.nanolett.3c03265.

All materials used in this study; the gel purification methods; the experimental procedures for preparation of DNA complexes; the methods for fluorescence measurements; and the typical operation for resetting behavior tests (PDF)

■ AUTHOR INFORMATION

Corresponding Authors

Haojun Liang − *Hefei National Research Center for Physical Sciences at the Microscale, Department of Polymer Science and Engineering, School of Chemistry and Materials Science, Collaborative Innovation Center of Chemistry for Energy Materials (iChEM), University of Science and Technology of China, Hefei, Anhui 230026, China;* orcid.org/0000-0002-7840-7586; Email: hjliang@ustc.edu.cn

Dongbao Yao − *Hefei National Research Center for Physical Sciences at the Microscale, Department of Polymer Science and Engineering, School of Chemistry and Materials Science, Collaborative Innovation Center of Chemistry for Energy Materials (iChEM), University of Science and Technology of China, Hefei, Anhui 230026, China;* orcid.org/0000-0003-4719-9726; Email: dbyao@ustc.edu.cn

Author

Xiaoyun Sun − *Hefei National Research Center for Physical Sciences at the Microscale, Department of Polymer Science and Engineering, School of Chemistry and Materials Science, Collaborative Innovation Center of Chemistry for Energy Materials (iChEM), University of Science and Technology of China, Hefei, Anhui 230026, China*

Complete contact information is available at: https://pubs.acs.org/10.1021/acs.nanolett.3c03265

Author Contributions

‡X.S. and D.Y. contributed equally to this work. D.Y. and H.L. conceived the project and designed the experiments. X.S. and D.Y. executed the experiments. D.Y. wrote the manuscript. All authors discussed the results and commented on the manuscript.

Notes

The authors declare no competing financial interest.

■ ACKNOWLEDGMENTS

This work was supported by the National Natural Science Foundation of China (Nos. 52003264, 21991132, and 52021002), the USTC Research Funds of the Double First-Class Initiative (YD2060002031), the National Key R&D Program of China (No. 2020YFA0710703), and the Open Research Fund of State Key Laboratory of Polymer Physics and Chemistry.

■ REFERENCES

(1) Seeman, N. C.; Sleiman, H. F. DNA Nanotechnology. *Nat. Rev. Mater.* **2018**, *3*, 17068.

(2) Zhang, D. Y.; Seelig, G. Dynamic DNA Nanotechnology Using Strand-Displacement Reactions. *Nat. Chem.* **2011**, *3*, 103−113.

(3) Yurke, B.; Turberfield, A. J.; Mills, A. P.; Simmel, F. C.; Neumann, J. L. A DNA-Fuelled Molecular Machine Made of DNA. *Nature* **2000**, *406*, 605−608.

(4) Simmel, F. C.; Yurke, B.; Singh, H. R. Principles and Applications of Nucleic Acid Strand Displacement Reactions. *Chem. Rev.* **2019**, *119*, 6326−6369.

(5) Thubagere, A. J.; Li, W.; Johnson, R. F.; Chen, Z.; Doroudi, S.; Lee, Y. L.; Izatt, G.; Wittman, S.; Srinivas, N.; Woods, D.; Winfree, E.; Qian, L. A Cargo-Sorting DNA Robot. *Science* **2017**, *357*, No. eaan6558.
(6) Yao, D.; Bhadra, S.; Xiong, E.; Liang, H.; Ellington, A. D.; Jung, C. Dynamic Programming of a DNA Walker Controlled by Protons. *ACS Nano* **2020**, *14*, 4007−4013.
(7) Jung, C.; Allen, P. B.; Ellington, A. D. A Stochastic DNA Walker That Traverses a Microparticle Surface. *Nat. Nanotechnol.* **2016**, *11*, 157−163.
(8) Srinivas, N.; Parkin, J.; Seelig, G.; Winfree, E.; Soloveichik, D. Enzyme-Free Nucleic Acid Dynamical Systems. *Science* **2017**, *358*, No. eaal2052.
(9) Chao, J.; Wang, J.; Wang, F.; Ouyang, X.; Kopperger, E.; Liu, H.; Li, Q.; Shi, J.; Wang, L.; Hu, J.; Wang, L.; Huang, W.; Simmel, F. C.; Fan, C. Solving Mazes with Single-Molecule DNA Navigators. *Nat. Mater.* **2019**, *18*, 273−279.
(10) Green, A. A.; Silver, P. A.; Collins, J. J.; Yin, P. Toehold Switches: De-Novo-Designed Regulators of Gene Expression. *Cell* **2014**, *159*, 925−939.
(11) Li, J.; Johnson-Buck, A.; Yang, Y. R.; Shih, W. M.; Yan, H.; Walter, N. G. Exploring the Speed Limit of Toehold Exchange with a Cartwheeling DNA Acrobat. *Nat. Nanotechnol.* **2018**, *13*, 723−729.
(12) Wang, F.; Lv, H.; Li, Q.; Li, J.; Zhang, X.; Shi, J.; Wang, L.; Fan, C. Implementing Digital Computing with DNA-Based Switching Circuits. *Nat. Commun.* **2020**, *11*, 121.
(13) Wilhelm, D.; Bruck, J.; Qian, L. Probabilistic Switching Circuits in DNA. *Proc. Natl. Acad. Sci. U.S.A.* **2018**, *115*, 903−908.
(14) Xie, N.; Li, M.; Wang, Y.; Lv, H.; Shi, J.; Li, J.; Li, Q.; Wang, F.; Fan, C. Scaling up Multi-Bit DNA Full Adder Circuits with Minimal Strand Displacement Reactions. *J. Am. Chem. Soc.* **2022**, *144*, 9479−9488.
(15) Xiong, X.; Xiao, M.; Lai, W.; Li, L.; Fan, C.; Pei, H. Optochemical Control of DNA-Switching Circuits for Logic and Probabilistic Computation. *Angew. Chem., Int. Ed.* **2021**, *60*, 3397−3401.
(16) Sun, X.; Wei, B.; Guo, Y.; Xiao, S.; Li, X.; Yao, D.; Yin, X.; Liu, S.; Liang, H. A Scalable "Junction Substrate" to Engineer Robust DNA Circuits. *J. Am. Chem. Soc.* **2018**, *140*, 9979−9985.
(17) Xiong, X.; Zhu, T.; Zhu, Y.; Cao, M.; Xiao, J.; Li, L.; Wang, F.; Fan, C.; Pei, H. Molecular Convolutional Neural Networks with DNA Regulatory Circuits. *Nat. Mach. Intell.* **2022**, *4*, 625−635.
(18) Qian, L.; Winfree, E.; Bruck, J. Neural Network Computation with DNA Strand Displacement Cascades. *Nature* **2011**, *475*, 368−372.
(19) Zhang, D. Y.; Turberfield, A. J.; Yurke, B.; Winfree, E. Engineering Entropy-Driven Reactions and Networks Catalyzed by DNA. *Science* **2007**, *318*, 1121−1125.
(20) Wu, C.; Cansiz, S.; Zhang, L.; Teng, I. T.; Qiu, L.; Li, J.; Liu, Y.; Zhou, C.; Hu, R.; Zhang, T.; Cui, C.; Cui, L.; Tan, W. A Nonenzymatic Hairpin DNA Cascade Reaction Provides High Signal Gain of mRNA Imaging inside Live Cells. *J. Am. Chem. Soc.* **2015**, *137*, 4900−4903.
(21) Li, X.; Yao, D.; Zhou, J.; Zhou, X.; Sun, X.; Wei, B.; Li, C.; Zheng, B.; Liang, H. Cascaded DNA Circuits-Programmed Self-Assembly of Spherical Nucleic Acids for High Signal Amplification. *Sci. China Chem.* **2020**, *63*, 92−98.
(22) Yao, D.; Song, T.; Sun, X.; Xiao, S.; Huang, F.; Liang, H. Integrating DNA-Strand-Displacement Circuitry with Self-Assembly of Spherical Nucleic Acids. *J. Am. Chem. Soc.* **2015**, *137*, 14107−14113.
(23) Zhou, X.; Yao, D.; Hua, W.; Huang, N.; Chen, X.; Li, L.; He, M.; Zhang, Y.; Guo, Y.; Xiao, S.; Bian, F.; Liang, H. Programming Colloidal Bonding Using DNA Strand-Displacement Circuitry. *Proc. Natl. Acad. Sci. U.S.A.* **2020**, *117*, 5617−5623.
(24) Yao, D.; Zhang, Y.; Zhou, X.; Sun, X.; Liu, X.; Zhou, J.; Jiang, W.; Hua, W.; Liang, H. Catalytic-Assembly of Programmable Atom Equivalents. *Proc. Natl. Acad. Sci. U.S.A.* **2023**, *120*, No. e2219034120.
(25) Amodio, A.; Adedeji, A. F.; Castronovo, M.; Franco, E.; Ricci, F. pH-Controlled Assembly of DNA Tiles. *J. Am. Chem. Soc.* **2016**, *138*, 12735−12738.
(26) Woods, D.; Doty, D.; Myhrvold, C.; Hui, J.; Zhou, F.; Yin, P.; Winfree, E. Diverse and Robust Molecular Algorithms Using Reprogrammable DNA Self-Assembly. *Nature* **2019**, *567*, 366−372.
(27) Song, T.; Xiao, S.; Yao, D.; Huang, F.; Hu, M.; Liang, H. An Efficient DNA-Fueled Molecular Machine for the Discrimination of Single-Base Changes. *Adv. Mater.* **2014**, *26*, 6181−6185.
(28) Yao, D.; Li, H.; Guo, Y.; Zhou, X.; Xiao, S.; Liang, H. A pH-Responsive DNA Nanomachine-Controlled Catalytic Assembly of Gold Nanoparticles. *Chem. Commun.* **2016**, *52*, 7556−7559.
(29) Jung, J. K.; Archuleta, C. M.; Alam, K. K.; Lucks, J. B. Programming Cell-Free Biosensors with DNA Strand Displacement Circuits. *Nat. Chem. Biol.* **2022**, *18*, 385−393.
(30) He, X.; Zeng, T.; Li, Z.; Wang, G.; Ma, N. Catalytic Molecular Imaging of microRNA in Living Cells by DNA-Programmed Nanoparticle Disassembly. *Angew. Chem., Int. Ed.* **2016**, *55*, 3073−3076.
(31) Liang, C.-P.; Ma, P.-Q.; Liu, H.; Guo, X.; Yin, B.-C.; Ye, B.-C. Rational Engineering of a Dynamic, Entropy-Driven DNA Nanomachine for Intracellular microRNA Imaging. *Angew. Chem., Int. Ed.* **2017**, *56*, 9077−9081.
(32) Garg, S.; Shah, S.; Bui, H.; Song, T.; Mokhtar, R.; Reif, J. Renewable Time-Responsive DNA Circuits. *Small* **2018**, *14*, No. 1801470.
(33) Eshra, A.; Shah, S.; Song, T.; Reif, J. Renewable DNA Hairpin-Based Logic Circuits. *IEEE Trans. Nanotechnol.* **2019**, *18*, 252−259.
(34) Tamba, M.; Murayama, K.; Asanuma, H.; Nakakuki, T. Renewable DNA Proportional-Integral Controller with Photoresponsive Molecules. *Micromachines* **2022**, *13*, 193.
(35) Nakakuki, T.; Murayama, K.; Asanuma, H. DNA Concentration Regulator That Can Be Driven for a Long Time. *New Gener. Comput.* **2022**, *40*, 681−702.
(36) Song, X.; Eshra, A.; Dwyer, C.; Reif, J. Renewable DNA Seesaw Logic Circuits Enabled by Photoregulation of Toehold-Mediated Strand Displacement. *RSC Adv.* **2017**, *7*, 28130−28144.
(37) Hahn, J.; Shih, W. M. Thermal Cycling of DNA Devices Via Associative Strand Displacement. *Nucleic Acids Res.* **2019**, *47*, 10968−10975.
(38) Pei, Y.; Bian, T.; Liu, Y.; Liu, Y.; Xie, Y.; Song, J. Single-Molecule Resettable DNA Computing Via Magnetic Tweezers. *Nano Lett.* **2022**, *22*, 3003−3010.
(39) Deng, J.; Walther, A. Fuel-Driven Transient DNA Strand Displacement Circuitry with Self-Resetting Function. *J. Am. Chem. Soc.* **2020**, *142*, 21102−21109.
(40) Idili, A.; Vallée-Bélisle, A.; Ricci, F. Programmable pH-Triggered DNA Nanoswitches. *J. Am. Chem. Soc.* **2014**, *136*, 5836−5839.
(41) Hu, Y.; Ren, J.; Lu, C.-H.; Willner, I. Programmed pH-Driven Reversible Association and Dissociation of Interconnected Circular DNA Dimer Nanostructures. *Nano Lett.* **2016**, *16*, 4590−4594.
(42) Hu, Y.; Cecconello, A.; Idili, A.; Ricci, F.; Willner, I. Triplex DNA Nanostructures: From Basic Properties to Applications. *Angew. Chem., Int. Ed.* **2017**, *56*, 15210−15233.
(43) Guo, Y.; Yao, D.; Zheng, B.; Sun, X.; Zhou, X.; Wei, B.; Xiao, S.; He, M.; Li, C.; Liang, H. pH-Controlled Detachable DNA Circuitry and Its Application in Resettable Self-Assembly of Spherical Nucleic Acids. *ACS Nano* **2020**, *14*, 8317−8327.
(44) Liu, D.; Balasubramanian, S. A Proton-Fuelled DNA Nanomachine. *Angew. Chem., Int. Ed.* **2003**, *42*, 5734−5736.
(45) Abou Assi, H.; Garavís, M.; González, C.; Damha, M. J. I-Motif DNA: Structural Features and Significance to Cell Biology. *Nucleic Acids Res.* **2018**, *46*, 8038−8056.
(46) Nesterova, I. V.; Nesterov, E. E. Rational Design of Highly Responsive pH Sensors Based on DNA I-Motif. *J. Am. Chem. Soc.* **2014**, *136*, 8843−8846.

https://doi.org/10.1021/acs.nanolett.3c03265
Nano Lett. 2023, 23, 11540−11547

(47) Leitner, D.; Schröder, W.; Weisz, K. Influence of Sequence-Dependent Cytosine Protonation and Methylation on DNA Triplex Stability. *Biochemistry* **2000**, *39*, 5886−5892.
(48) Qian, L.; Winfree, E. Scaling up Digital Circuit Computation with DNA Strand Displacement Cascades. *Science* **2011**, *332*, 1196−1201.
(49) Cherry, K. M.; Qian, L. Scaling up Molecular Pattern Recognition with DNA-Based Winner-Take-All Neural Networks. *Nature* **2018**, *559*, 370−376.
(50) Zhang, D. Y.; Winfree, E. Control of DNA Strand Displacement Kinetics Using Toehold Exchange. *J. Am. Chem. Soc.* **2009**, *131*, 17303−17314.
(51) Li, B.; Ellington, A. D.; Chen, X. Rational, Modular Adaptation of Enzyme-Free DNA Circuits to Multiple Detection Methods. *Nucleic Acids Res.* **2011**, *39*, e110−e110.
(52) Chen, X.; Briggs, N.; McLain, J. R.; Ellington, A. D. Stacking Nonenzymatic Circuits for High Signal Gain. *Proc. Natl. Acad. Sci. U.S.A.* **2013**, *110*, 5386−5391.
(53) Zhang, D. Y.; Winfree, E. Robustness and Modularity Properties of a Non-Covalent DNA Catalytic Reaction. *Nucleic Acids Res.* **2010**, *38*, 4182−4197.
(54) Jiang, Y. S.; Bhadra, S.; Li, B.; Ellington, A. D. Mismatches Improve the Performance of Strand-Displacement Nucleic Acid Circuits. *Angew. Chem., Int. Ed.* **2014**, *53*, 1845−1848.
(55) Wang, S.; Lee, S.; Du, J. S.; Partridge, B. E.; Cheng, H. F.; Zhou, W.; Dravid, V. P.; Lee, B.; Glotzer, S. C.; Mirkin, C. A. The Emergence of Valency in Colloidal Crystals through Electron Equivalents. *Nat. Mater.* **2022**, *21*, 580−587.
(56) Ke, Y.; Ong, L. L.; Shih, W. M.; Yin, P. Three-Dimensional Structures Self-Assembled from DNA Bricks. *Science* **2012**, *338*, 1177−1183.

https://doi.org/10.1021/acs.nanolett.3c03265
Nano Lett. 2023, 23, 11540−11547